Anna Szynkiewicz
Department of Earth & Planetary Sciences, University of Tennessee,
corresponding author: aszynkie@utk.edu

Magdalena Modelska
Institute of Geological Sciences, University of Wrocław,
corresponding author: magdalena.modelska@ing.uni.wroc.pl

Miguel Rangel Medina
Department of Geology, University of Sonora

G. Lang Farmer
Department of Geological Sciences and CIRES, University of Colorado

Pedro Hernandez Rabago
Mexican Geological Survey_NW

Rogelio Monreal
Department of Geology, University of Sonora

Age and shape of paleo-seawater intrusions in the semi-arid coastal aquifer of Sonora Desert, northern Mexico

Abstract

The Costa de Hermosillo aquifer has been contaminated by paleo-seawater intrusions over a distance of ~20–32 km from the modern coastline of the Gulf of California due to over pumping of the aquifer for agricultural purposes. In the most contaminated portion of this aquifer, the paleo-seawater intrusions were characterized by high values of electric conductivity (3.3 to 41.7 mS/cm), higher $\delta^{2}H$ and $\delta^{18}O$ values of water (–6.1 to –1.0 ‰ and –45 to –18 ‰ respectively), sulfate depletion (down to < 1 mg/L) and high $\delta^{34}S$ values of sulfate (+20.0 to +32.0 ‰) similar as found in marine sediments with active zones of microbial sulfate reduction. The salinization appears to be caused by mobilization of the relicts of paleo-seawater residing in the blue clays strata deposited during the Mio-Pliocene transgression. The paleo-seawater had lower $^{87}Sr/86Sr$ ratio (0.708326) compared to modern seawater of the Gulf of California (0.709181) which is indicative of groundwater-rock interaction during a long residence time of paleo-seawater in the aquifer.

Geoscience Notes 2.2, 2014

At present, the paleo-seawater intrusions show different stages of dilution by meteoric water and occur in the form of saline lenses that reside at the current groundwater table of ~ –30 meters. The spatial, stratigraphic and geochemical relationships suggest that lithospheric deformation, related to the opening of the Gulf of California, led to isolation of some portions of the Mio-Pliocene seawater in the studied aquifer and prevented subsequent flashing out by freshwater recharge in the subsequent events. Tectonic subsidence is likely an important factor controlling the storage of paleo-seawater wedges in the rift-type coastal aquifers.

Streszczenie

Ze względu na przeeksploatowanie warstw wodonośnych do celów rolniczych, zbiornik wód podziemnych Costa de Hermosillo został zdegradowany przez wystąpienie intruzji wód reliktowych pochodzenia morskiego, w odległości ~ 20–32 km od linii brzegowej Zatoki Kalifornijskiej. W najbardziej zmienionej części tego zbiornika, wody intruzji cechowały wysokie wartości przewodności elektrycznej właściwej (3,3 do 41,7 mS/cm), wysokie wartości $\delta^{2}H$ i $\delta^{18}O$ cząsteczki wody (odpowiednio –6,1 do –1,0 ‰ i –45 do –18 ‰), spadek stężeń siarczanów (do < 1 mg/l) i wysokie wartości $\delta^{34}S$ w jonie siarczanowym (20,0 do 32,0 ‰), jakie notuje się dla osadów morskich z aktywnymi strefami mikrobilogicznej redukcji siarczanu. Zasolenie wód spowodowane zostało prawdopodobnie przez mobilizację wód reliktowych z warstw niebieskich łupków zdeponowanych podczas transgresji mioceńsko-plioceńskiej. Wody reliktowe pochodzenia morskiego wykazywały niższy współczynnik $^{87}Sr/^{86}Sr$ (0,708326) w porównaniu ze współczesną wodą morską Zatoki Kalifornijskiej (0,709181), co wskazuje na oddziaływanie woda–skała podczas długiej stagnacji tych wód w warstwie wodonośnej.

Obecnie poszczególne intruzje wód reliktowych są efektem różnych etapów ich rozcieńczenia przez wody pochodzenia meteorycznego i występują w postaci soczewek solankowych towarzyszących wodom zwykłym, które lokalizują się w na głębokości ok. –30 metrów. Relacje przestrzenne, stratygraficzne i geochemiczne wskazują, że deformacje litosfery, związane z otwieraniem się Zatoki Kalifornijskiej, doprowadziły do izolacji części wody morskiej wieku mioceńsko-plioceńskiego w badanym zbiorniku wód podziemnych i zapobiegły, w późniejszym czasie, usunięciu ich z sytemu wodonośnego przez zasilanie wodami zwykłymi. Zjawiska tektoniczne mogą być więc istotnym czynnikiem kontrolującym retencję wód reliktowych w przybrzeżnych zbiornikach wód podziemnych o genezie ryftowej.

Keywords: paleo-seawater intrusion, sulfur and strontium isotopes, coastal aquifer, Gulf of California

1. Introduction

Salinization of groundwater resources is a challenging environmental problem of global importance that has been threatening many developed coastal regions across the world (e.g., Kohout 1960; Schmorak 1967; Giménez and Morell 1997; Steinich et al. 1998; Conti et al. 2000; Monreal et al. 2000; Daesslé et al. 2004; Werner and Gallagher 2006; Ma et al. 2006; Rangel-Medina 2006; Lee and Song 2007; Akouvi et al. 2008; Szynkiewicz et al. 2008; Han et al. 2011; Werner et al. 2013; Giménez-Forcada 2014). An extensive contamination by intrusion of saline waters results from broad exploitation of coastal aquifers for domestic, agricultural and industrial purposes.

This process reduces water quality and in some areas involves land subsidence, caused by lowering of the porewater pressures in the aquifers, due to over pumping of the resources (e.g. Conti et al. 2000). A nature of groundwater salinization is complex and widely controlled by proximity to the sea, climate, aquifer geometry, agriculture and geochemical character of different rock units.

A seawater intrusion is likely a main cause of salinization of freshwater coastal aquifers across the world. The extent of seawater intrusions greatly varies and depends on local geological and hydrological factors. In a distance of 100 m to 4 km from the modern coastlines, seawater intrusions most likely result from inland migration of saline/freshwater interface that defines a mixing zone between natural freshwater recharge from the continents and seawater front (Kohout 1960; Schmorak 1967; Nadler et al. 1980; Mercado 1985; Magaritz and Luzier 1985; Bond and Bredehoeft 1987; Giménez and Morell 1997; Konikow and Reilly 1999; Melloul and Zeitoun 1999; Martínez and Bocanegra 2002; Kim et al. 2003ab; Demirel 2004; Panagopoulos et al. 2004; Capaccioni et al. 2005; Sivan et al. 2005; Ghabayen et al. 2006; Giambastiani et al. 2007; Lee and Song 2007; Duque et al. 2008; Custodio 2010; Steyl and Dennis 2010; Werner 2010; Werner et al. 2013). The lateral movement of seawater due to leakage through offshore outcrops has been enhanced by the extensive extraction of fresh groundwater and global changes of sea level. In some coastal areas, the intrusions of seawater have occurred further inland within 8 to 15 km from the coastline (Hussein 1982; Arakel and Ridley 1986; Sadeg and Karahanoğlu 2001; Vengosh et al. 2002; Werner and Gallagher 2006; Petalas and Lambrakis 2006; Fass et al. 2007; Werner et al. 2013); however, the origin of these intrusions is often inconclusive, thus, incursion of paleo-seawater (also called relict/fossil seawater or connate/formation water) has been indicated as another important factor (Vengosh et al. 1994a; Akouvi et al. 2008). Less common are reports on seawater intrusions occurring 20 to 32 km inland with limited information on their ages and origin (e.g., Post et al. 2003; Ma et al. 2006; Akouvi et al. 2008; Szynkiewicz et al. 2008).

Usually, inland seawater intrusions show a varied degree of alteration compared to modern seawater; this mainly relates to different processes such as cation exchange enhanced by seawater-rock interaction (e.g., Nadler et al. 1980; Magaritz and Luzier 1985; Panagopoulos et al. 2004), microbial sulfate reduction involving sulfate removal (e.g., Magaritiz and Luzier 1985; Martínez and Bocanegra 2002; Capaccioni et al. 2005; Szynkiewicz et al. 2008), and evaporation of seawater prior to burial (e.g., Rosenthal et al. 2006).

Climate is an important factor controlling the extent of salinization by seawater in coastal regions since the freshwater recharge acts as a driving force of moving the saline/freshwater interface seaward and flashing out of saline horizons from former sea transgressions. The most stressed regions are arid and semi-arid coastal aquifers because of limited precipitation that enhances slow recharge rates and decreases natural renewal of groundwater resources in the already over pumped aquifers. In addition

to the problem of climate, the arid coastal regions may be threatened by incursion of unflashed portions of paleo-seawater which were trapped in coastal sediments during former sea transgressions; however, our knowledge of the ages, locations and mobility of paleo-seawater is limited (e.g., Jones et al. 1999; Werner and Gallagher 2006).

The Costa de Hermosillo aquifer of Sonora Desert (Figure 1) is one semi-arid coastal aquifer that is likely contaminated by seawater intrusions as a result of intensive agricultural activity supported by coastal groundwater for over 60 years (Steinich et al. 1998; Rangel-Medina et al. 2004; Szynkiewicz et al. 2008). In this area, the seawater intrusions are interesting phenomena because they occur ~20–32 km inland from the modern coastline of the Gulf of California (II Anomaly in Figure 1) and cannot be easily explained by moving of the modern saline/freshwater interface within the aquifer as suggested for other coastal areas across the world. The incursion of seawater occurred relatively fast in this aquifer, during the first 10 to 15 years of agriculture operations (Miller 1994; Halvorson et al. 2003), and currently, this portion of the aquifer is excluded from agricultural activity. The seawater encroachment has not changed the policy of agricultural expansion and the groundwater pumping continues a few kilometers northward and eastward from the seawater intrusions. The ongoing pumping has likely caused a formation of another saline anomaly over the years (I Anomaly in Figure 1); however, no detailed study has been undertaken to describe the source of new saline water and whether the groundwater is threatened by the same extent of salinization as observed in the already contaminated portions of the aquifer.

Preliminary study presented by Szynkiewicz et al. (2008) indicated that seawater intrusions in the Costa de Hermosillo aquifer likely resulted from the incursion of paleo-seawater trapped in the aquifer sometime in the past. In order to better explain the age and shape of paleo-seawater intrusions in different parts of this aquifer, we used the multiple isotope (Sr, S, H, O) and chemical (SO_4^{2-}, Cl^-, HCO_3^-, Br^-, Ca^{2+}, Mg^{2+}, Na^+, K^+) tracers. New groundwater samples were taken in November 2007 from several wells within I and II Anomalies. Vertical measurements of isotope and chemical compositions in the abandoned wells with paleo-seawater intrusions, combined with field observations and technical parameters of extraction wells, allowed us to elucidate a spatial relationship between paleo-seawater intrusions in both anomalies and define major factors controlling the mobility of paleo-seawater intrusions in the rift-type coastal aquifer.

2. Study area

The Costa de Hermosillo aquifer is located southwest of the City of Hermosillo along the northeastern coastline of the Gulf of California (Figure 1). This region has a dry climate with average annual temperature varying from 22 to 24°C. Rain mainly falls from June to September, with peak precipitation in July and August varying from 75 to 200 mm/year. The aquifer resides within a sedimentary graben formed during crustal

extension related to opening of the Gulf of California and is characterized by NW-SE to NE-SW oriented normal faults (Csérna de 1989). The sediment thickness in the graben varies mostly from 150 to 500 m in depth but locally reaches 800 m in depth (Rangel-Medina et al. 2002). Two aquifers are recognized in the western Costa de Hermosillo. A marine sedimentary sequence (blue clay) consisting of clay and limestone with a marine fauna separates both aquifers (Monreal et al. 2000). The blue clay was deposited during Miocene/Pliocene marine transgression. The thickness of the blue clay is approximately 400 m near the coast, pinching out towards the northeast. About 40 km from the coast, the blue clay disappears and the two aquifers coalesce. The upper aquifer is 100 to 560 m thick and resides in Miocene and younger silt, sand, and gravel. The upper aquifer hosts about 500 wells and is intensively pumped for groundwater resources. The lower aquifer averages 350 m in thickness and resides in Miocene deposits consisting of sandstone and gravel which overly the faulted basement.

During the first 20 years of agricultural operations (1947–1967), groundwater pumping caused the progressive formation of a wide depression cone. Piezometric levels near the pumping center reached 65 m below sea level in 2001 (Rangel-Medina et al. 2003). From 2001 to 2007, stabilization of the depth of depression cone and diameter was observed. Most pronounced salinization took place on the western/coastal side of the aquifer during the first 10–15 years of pumping (II Anomaly in Figure 1). The salinization apparently resulted from the upward intrusion of paleo-seawater trapped as pore water in the Miocene/Pliocene blue clays underlying the upper aquifer (Szynkiewicz et al. 2008). Two other saline anomalies (I and III Anomaly in Figure 1), showing much less salinization (Steinich et al. 1998), are aligned roughly parallel to the coastline and are located at approximately the same distance from the sea as the already recognized intrusion of paleo-seawater (Figure 1).

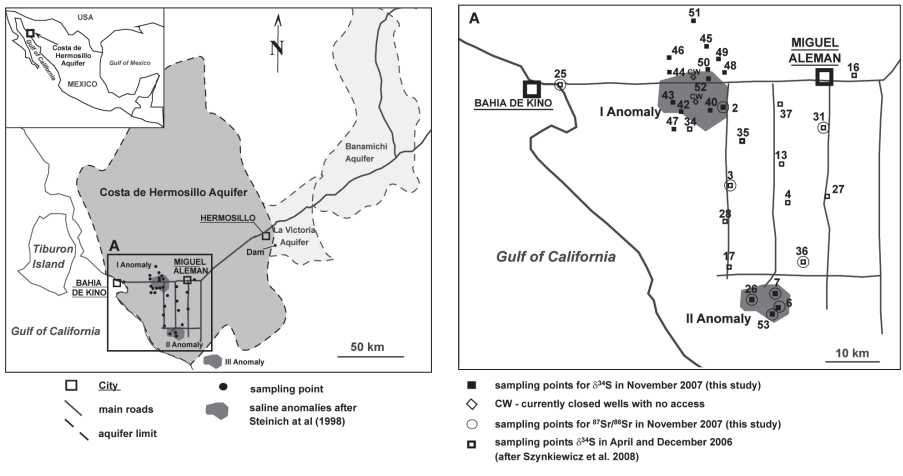

Figure 1. Location of the study area with the groundwater sampling sites in the Costa de Hermosillo aquifer. The position of three saline anomalies (I, II and III) are shown based on distribution of Na/Cl × 1000 measured by Steinich et al. (1998)

Additionally, the Costa de Hermosillo aquifer has been polluted by a broad application of fertilizers on cultivated land that led to the large contamination of groundwater by nitrates and nitrites (Steinich et al. 1998; Szynkiewicz et al. 2008), and increased sulfate contents in the drainage zone (Szynkiewicz et al. 2008). The latter is apparently caused by addition of $(NH_4)_2SO_4$ fertilizers and/or weathering of magmatic sulfides enhanced by artificial oxygenation of the aquifer due to prolonged flood irrigation and pumping.

3. Methods

3.1. Field sampling

In November 2007, groundwater was collected from 13 wells used for irrigation on farms in which elevated chloride contents were reported (I Anomaly in Figure 1). All wells were operated by farmers and the pumped water was sampled directly into plastic bottles. Wells are 100–200 m (most common 160 m) long and are screened along the entire length.

A vertical sampling was carried out on three abandoned wells (no. 7, 26, 53) for which pumping devices were removed after first evidence of salinization resulted from intrusion of paleo-seawater in II Anomaly (Figure 1). These wells are 53–67 m long, screened along the entire length, with the current water table ~30 m beneath the surface. As they were abandoned about 50 years ago, it was assumed that they likely represent an equilibrated system for vertical measurements of chemical and isotope parameters. In fact, the water table of Well 7 showed negligible seasonal variations of chemical and isotope compositions along 2006 (Szynkiewicz et al. 2008). The chemical and isotope composition of Wells 26 and 53 have not been reported yet; they are situated about 2 km southwest and south from Well 7, respectively (Figure 1A).

For all abandoned wells, groundwater was sampled using hand operated sampler of 500 ml capacity with a self-releasing locker activated by dropping down the rope a stainless steel cylinder. Water samples were taken from three depths: –30 m (water table), –40 m and –67 m for Well 7, –31 m (water table), –41 m and –61 m for Well 26, and –34 m (water table), –44 m and –53 m for Well 53.

3.2. Chemical analysis

Concentrations of HCO_3^- were measured as total alkalinity directly in the field. A 100 mL of water sample was used for titration using 0.05 M HCl in the presence of methyl orange. The alkalinity, in meq units, was calculated using the gram-equivalent of HCO_3^-. The analytical precision was better than < 3 mg/L. Concentrations of SO_4^{2-}, Cl^- and Br^- were measured after returning to the labo-

ratory using a Dionex ICS-2000 ion chromatograph with a 30 mM KOH eluent controlled by an eluent generator. Anions were run on an IonPac®AS11-HC ion exchange column. Concentrations of Ca^{2+}, Mg^{2+}, Na^{+} and K^{+} were measured using a Perkin Elmer Analyst 800 atomic absorption spectrometer with the hollow cathode lamps and run on flame analyzer using standard methods. For accurate analysis of cations and anions, water samples were diluted in a 1:10, 1:100, 1:1000 or 1:10000 ratios using NanoPure Water from a Millipore Gradient Mili-Q Water filtration system with Quantum™EX and Q-Gard®-2 dual filtration system with UV treatment. During the handling of samples for the Sonora study, laboratory NanoPure water had conductivity of 0.055 μS/cm. The overall analytical precision of chemical analysis was 1% for groundwater from the I Anomaly and 17% for highly mineralized samples from abandoned wells located within the II Anomaly.

Water electric conductivity was measured directly in the field using a La Motte Con 5 Mater that was one-point calibrated with a solution of 1413 μS/cm.

3.3. Sulfur, oxygen and hydrogen isotope analysis

A method of samples preparation for sulfur isotope analyses of sulfates was the same as in Szynkiewicz et al. (2008). Sulfur isotopic compositions of sulfate were determined using an EA1110 elemental analyzer coupled to a Finnigan Mat 252 isotope ratio mass spectrometer via a ConFlo II split interface in a Stable Isotope Research Facility (SIRF) at Indiana University. Isotopic data are reported with respect to VCDT (Vienna Cañon Diablo Troilite). Analytical reproducibility was better than 0.2‰.

Hydrogen and oxygen isotope composition of waters were analyzed using a Hydrogen Device and Gas Bench in SIRF-Indiana, respectively (e.g., Brand et al. 1996; Horita et al. 1989). Isotopic data are reported with respect to VSMOW (Vienna Standard Mean Ocean Water) and raw data were calibrated relative to the SMOW and SLAP (Standard Light Antarctic Precipitation) standards. Analytical reproducibility was better than 1 ‰ for $\delta^{2}H$ and 0.2‰ for $\delta^{18}O$ values.

3.4. Strontium isotope analysis

In total, 10 samples of groundwater were taken for strontium isotope analysis in November of 2007 (Figure 1). For abandoned wells in II Anomaly (no. 7, 26, 53), groundwater samples were taken using hand-operated bailer near the groundwater table and these samples were sampled prior to vertical sampling along the water column (SR-5, -3, -2; Table 4). Additionally, one groundwater sample was taken from Well 25 (SR-4) located about 300 m from the coastline of the Gulf of California; this well has been shown to be entirely contaminated by modern seawater (Szynkiewicz et al. 2008).

Five samples were obtained from fresh groundwater at the active farms in I Anomaly (Well 2; SR-9), II Anomaly (Well 6; SR-36), and the uncontaminated portion of the aquifer (Wells 3, 31, 36; SR-7, -8, -6). One sample (SR-10) of surface water was taken from the Hermosillo Dam located a few kilometers southeastward from the City of Hermosillo (Figure 1).

Strontium was separated from the groundwater samples using SrSpec® resin in a Class 100 clean room environment at the University of Colorado, Boulder. Isotopic measurements were carried out on a six-collector, Finnigan-MAT thermal ionization mass spectrometer. Analytical details are given in Table 4.

4. Results

4.1. Chemical analysis

For I Anomaly, relatively low sulfate concentrations were observed, 35 to 153 mg/L, compared to considerably high values of chloride concentrations, 15 to 1482 mg/L (Table 1). In regional scale, chloride concentrations showed concentric pattern of increasing values in the center of I Anomaly, similarly as it was observed for II Anomaly (Figure 2). In contrast to II Anomaly, sulfate concentrations did not show the distinctive spatial distribution within I Anomaly and varied in the same range such as observed for uncontaminated portion of the Costa de Hermosillo aquifer (Figure 3).

For II Anomaly, the abandoned wells showed broad variations in sulfate and chloride concentrations. Well 7 had largest variations of sulfate and chloride concentrations in vertical scale (Table 2, Figure 4); sulfate concentrations increased with depth from 148 mg/L (–30 m, water table) to 5,772 (–40 m) and 7,166 mg/L (–67 m). Similarly, the chloride concentrations increased from 10,649 mg/L (–30 m) to 64,976 (–40 m) and 67,779 mg/L (–67 m) followed by the increase of electric conductivity, from 17.9 mS/cm (–30 m) to 32.4 (–40 m) and 41.7 mS/cm (–67 m). In contrast to Well 7, Wells 26 and 53 had lower chloride concentrations and sulfate below detection limit. For Well 26 chloride concentrations increased from 41,146 mg/L (–31 m, water table) to 44,176 (–41 m) and 46, 949 mg/L (–61 m), however, the electric conductivity had the same value of 26.4 mS/cm along the entire water column. For Well 53, chloride concentrations increased from 1,037 mg/L (–34 m, water table) to 1,542 (–44 m) and 3,497 mg/L (–53 m) followed by increase of electric conductivity, from 3.3 (–34 m) and 3.2 mS/cm (–44 m) to 6.6 mS/cm (–53 m).

Table 1. Variations of chemical composition (sulfate, chloride, bicarbonate, calcium, magnesium, sodium, potassium), $d^{34}S$ value of sulfate, and $d^{2}H$-$d^{18}O$ values for groundwater samples taken from active farms in November of 2007. n.a. – not analyzed.

Well No.	Well Name	SO_4 [mg/L]	Cl [mg/L]	HCO_3^- [mg/L]	Ca^{2+} [mg/L]	Mg^{2+} [mg/L]	Na^+ [mg/L]	K^+ [mg/L]	$d^{34}S(SO_4)$ [‰]	$d^{18}O(H_2O)$ [‰]	$d^{2}H(H_2O)$ [‰]
2	Valle Grande	68	1105	153	339	38	650	30	5.4	-6.5	-51
6	Campo Cuatro 1	47	339	78	149	17	90	3	9.1	n.a.	n.a.
40	Uruapan	86	629	122	168	28	85	5	5.9	-6.2	-49
42	San Alfonso	63	103	177	46	9	47	3	2.8	-6.3	-49
43	Santa Anita	39	1482	159	301	73	137	8	4.4	-6.4	-49
44	San Antonio	139	538	122	170	27	66	5	0.8	-6.3	-51
45	Navolato	45	13	177	29	7	44	3	1.4	-6.4	-50
46	El Kilowat	153	453	195	161	29	75	5	1.8	-6.2	-49
47	San Ignacio	29	129	174	60	6	61	4	1.3	-6.0	-46
48	El Enrique	107	55	146	97	16	59	3	1.3	-6.4	-51
50	San Ramon	44	24	232	35	7	41	3	1.5	-6.3	-49
51	San Alfonso 2	35	360	207	147	24	64	5	1.6	-5.7	-45
52	San Jose	46	326	122	149	17	90	3	2.3	-6.4	-50

Table 2. Vertical variations of electric conductivity, chemical composition (sulfate, chloride, bicarbonate, calcium, magnesium, sodium, potassium), $d^{34}S$ value of sulfate, and $d^{2}H$-$d^{18}O$ values for groundwater samples taken from abandoned wells (II Anomaly) in November of 2007. n.a. – not analyzed, b.d. – below detection.

Well No.	Well Name	Depth [m]	EC [mS/cm]	SO_4 [mg/L]	Cl [mg/L]	HCO_3^- [mg/L]	Ca^{2+} [mg/L]	Mg^{2+} [mg/L]	Na^+ [mg/L]	K^+ [mg/L]	$d^{34}S(SO_4)$ [‰]	$d^{18}O(H_2O)$ [‰]	$d^{2}H(H_2O)$ [‰]
7	Campo Dec	-30	17.9	148	10649	696	718	700	6484	77	32.0	-1.2	-18
		-40	32.4	5772	64976	n.a.	n.a.	n.a.	n.a.	n.a.	23.2	-1.4	-18
		-67	41.7	7166	67779	n.a.	1920	1430	9140	57	20.0	-1.0	-17
26	MD-05	-31	26.4	b.d.	41146	35	2574	445	2488	105	b.d.	-4.4	-40
		-41	26.4	b.d.	44176	n.a.	3313	561	2700	118	b.d.	-4.4	-37
		-61	26.4	b.d.	46946	n.a.	3303	550	2780	119	b.d.	-4.4	-40
53	Campo Cuatro 2	-34	3.3	b.d.	1037	81	151	18	197	38	b.d.	-6.1	-45
		-44	3.2	b.d.	1542	n.a.	166	22	270	41	b.d.	-5.9	-45
		-53	6.6	b.d.	3497	n.a.	505	76	421	38	b.d.	-5.7	-45

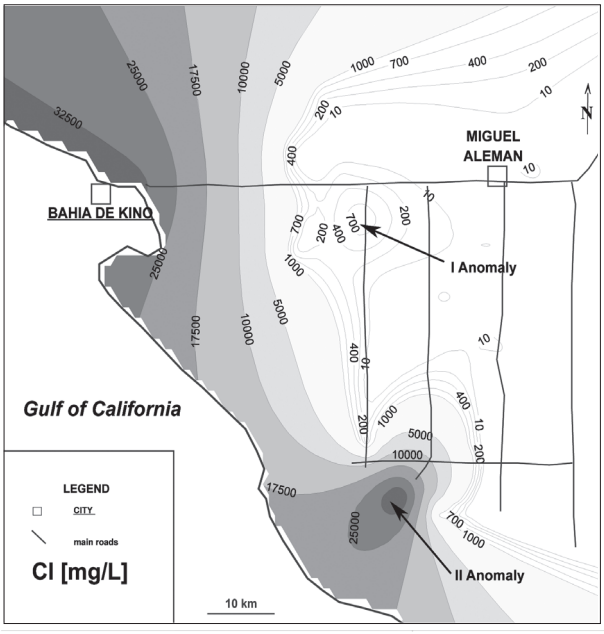

Figure 2. Distribution of chloride concentration in the groundwater from active farms and abandoned wells within I and II Anomalies. A kriging interpolation was used to show the spatial distribution of chloride concentration. The same method was used in Figures 3 and 5. For Wells 7, 26 and 53, the chloride concentration at depths of current water table (~ –30 m) was included in kriging. Locations of sampling points for kriging interpolation are shown in Figure 1.

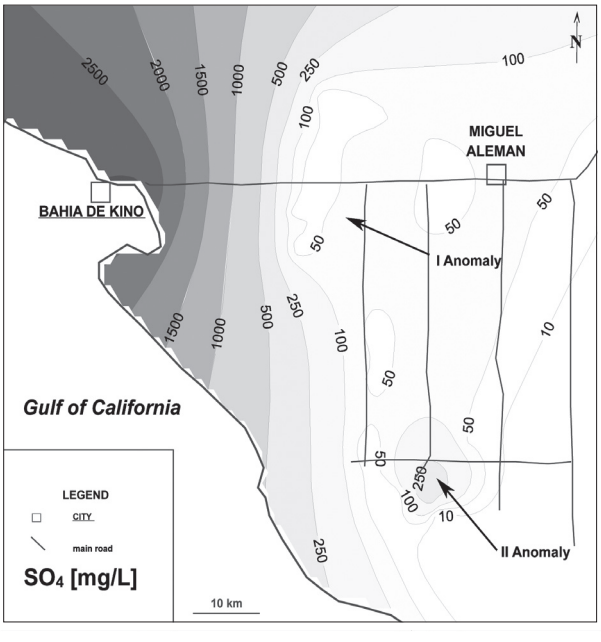

Figure 3. Distribution of sulfate concentration in the groundwater from active farms and abandoned wells within I and II Anomalies. For Well 7, the sulfate concentration at depth of current water table (~ –30 m) was included in kriging interpolation. Wells 26 and 53 were excluded from kriging because of the sulfate being below detection limit (< 1 mg/L). Locations of sampling points for kriging interpolation are shown in Figure 1

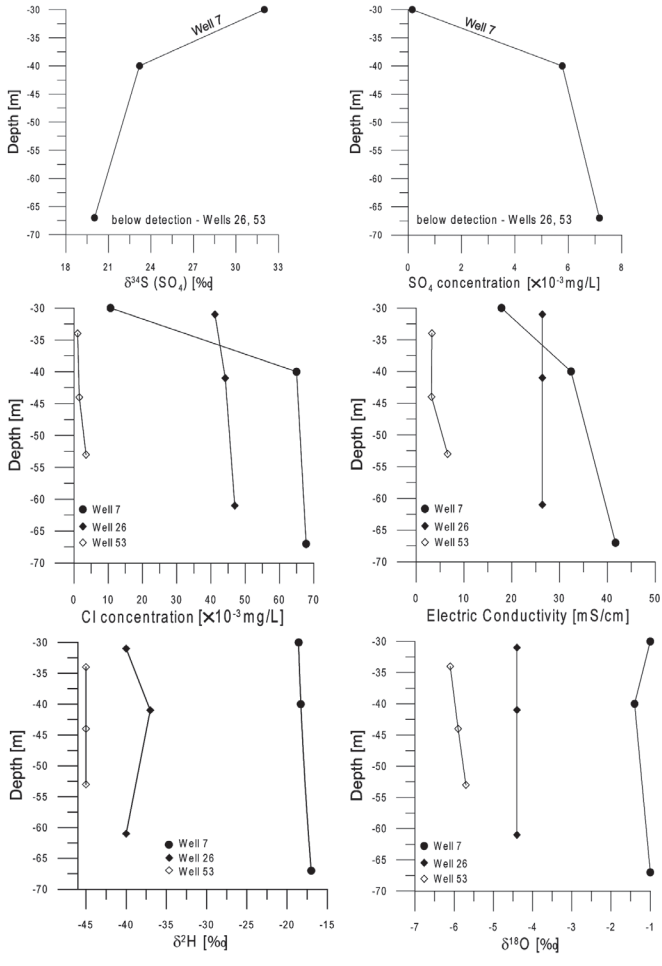

Figure 4. Variations of $\delta^{34}S$ of sulfate, chloride and sulfate concentrations, electric conductivity, and $\delta^{2}H$-$\delta^{18}O$ values along the groundwater column of the abandoned wells (II Anomaly). The well depth was measured relative to the topographic surface. In the time of sampling (November of 2007), the groundwater table was present at depths of –34 to –30 m

4.2. Sulfur, Oxygen and Hydrogen isotope analyses

For I Anomaly, $d^{34}S$ values of sulfate varied in narrow range, from +0.8 to +5.9 ‰ and were considerably lower compared to $d^{34}S$ values of +33 ‰ in the center of II Anomaly (Table 1, Figure 5). The $d^{34}S$ showed concentric pattern of increasing values in the center of I Anomaly, similarly as it was observed for II Anomaly (Figure 5). The $d^{18}O$ and $d^{2}H$ values varied in narrow range, –6.5 to –5.7 ‰ and –51 to –46 ‰ (Table 1), respectively, and were similar, such as observed for uncontaminated portion of the Costa de Hermosillo aquifer, –7.2 to 5.4 ‰ and –63 to –42 ‰ (Szynkiewicz et al. 2008).

For II Anomaly, considerably higher values of $\delta^{34}S$ were noted (Table 2, Figures 4, 5). The $\delta^{34}S$ values decreased with depth for Well 7, from +32.4 ‰ (–30 m) to +23.2 (–40 m) and +20.0 ‰ (–67 m). For Wells 26 and 53, $\delta^{34}S$ values were below detection limit. The $\delta^{18}O$ and $\delta^{2}H$ values widely varied between abandoned wells; from –1.4 to –1.0 ‰ and –33 to –17 ‰, respectively, for Well 7, –4.4 ‰ and –40 to –37 ‰ for Well 26, –6.1 to –5.7 ‰ and –45 ‰ for Well 53.

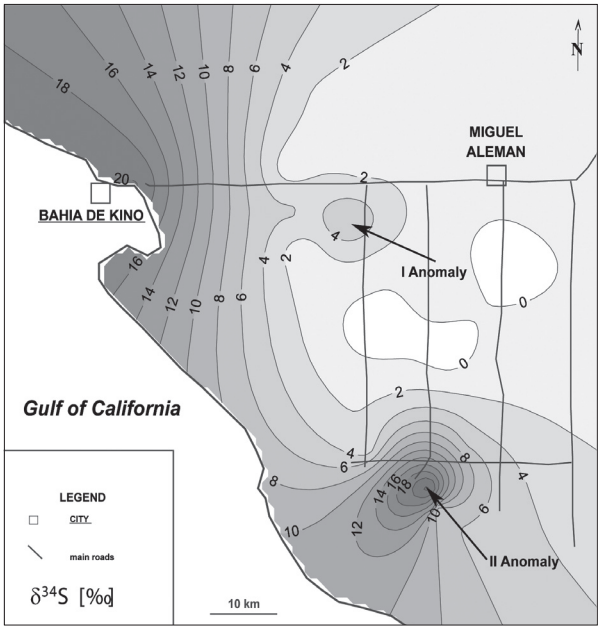

Figure 5. Spatial distribution of $\delta^{34}S$ values of sulfate in the groundwater from active farms and abandoned wells within I and II Anomaly. For Well 7, the $\delta^{34}S$ of sulfate at depth of current water table (~ –30 m) was included in kriging interpolation. Wells 26 and 53 were excluded from kriging because of the sulfate being below detection limit. Locations of sampling points used for kriging interpolation are shown in Figure 1

4.3. Strontium isotopes

With the exception of the sample from Well 25, which has a distinctively high $^{87}Sr/^{86}Sr$ value (0.709181), all of the water samples have similar measured $^{87}Sr/^{86}Sr$ values ranging from a low of 0.708196 (Well 3) to a high of 0.708355 (Well 2). Among these samples, there is no obvious correlation between the water Sr isotopic composition and concentration (Figure 6, Table 4).

Table 3. Strontium concentration and isotopic compositions for groundwater at selected active and abandoned farms. Sampled in November, 2007.

Sample	Well #	Sr (ppm) §	$^{87}Sr/^{86}Sr$ ±2σ †
SR-1	6	1.4	0.70831±13
SR-2	53	2.3	0.708215±13
SR-3	26	19	0.708273±9
SR-4	25	11	0.709181±11
SR-5	7	5.4	0.708326±12
SR-6	36	2.9	0.708316±15
SR-7	3	0.44	0.708196±16
SR-8	31	0.41	0.708317±16
SR-9	2	2.5	0.708355±6
SR-10	12	0.32	0.708325±14

§ - Sr concentrations by isotope dilutions, external reproducibilities estimated at ~1%

† - $^{87}Sr/^{86}Sr$ ratios were analyzed using four-collector static mode measurements. Thirty measurements of SRM-987 during study period yielded mean $^{87}Sr/^{86}Sr$=0.71032+/- 2. 2σ errors refer to last two digits of the $^{87}Sr/^{86}Sr$ ratio.

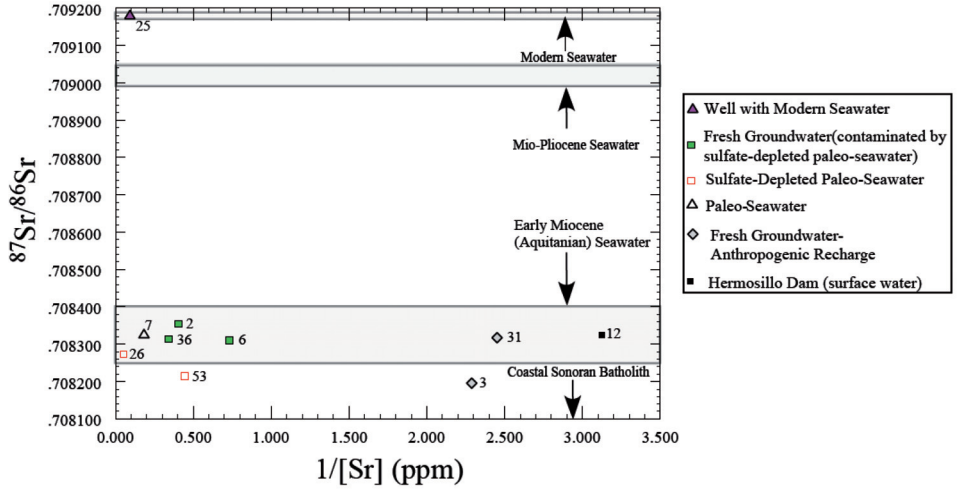

Figure 6. Measured Sr/ Sr vs. 1/[Sr] (ppm) for various well waters. The ranges of strontium isotope compositions for seawater of various ages from McArthur et al. (2001). The Coastal Sonoran Batholith strontium isotope compositions from Valencia-Moreno et al. (2003). Numbers on diagram refer to well designations (see location map in Figure 1)

5. Discussion

5.1. Diversity of paleo-seawater in II Anomaly

Previous study showed that the saline intrusion in II Anomaly was likely derived from paleo-seawater (Well 7) that was trapped as a pore water in the lower parts of the Costa

de Hermosillo aquifer (Szynkiewicz et al. 2008). The upward migration of paleo-seawater resulted from the lowering of the groundwater table due to overpumping of groundwater resources. The new chemical results from sampling in November of 2007 plotted in the Chebotarev diagram (Figure 7) demonstrate that there is another type of saline groundwater (Wells 26 and 53) within II Anomaly which show different chemical and isotope compositions compared to the paleo (Well 7) and modern (Well 25) seawater. This saline groundwater is characterized by lower mineralization (Table 2), slightly different proportions of cations compared to the paleo and modern seawater (Figure 7), the negative $d^{18}O$-$d^{2}H$ values representative for inland meteoric precipitation (Figure 8), and essential depletion in sulfate ions down to <1 mg/L (Table 2). Both the paleo-seawater (Well 7) and the sulfate-depleted saline groundwater (Wells 26, 53), however, appear to be closely situated on the Chebotarev diagram (Figure 7) suggesting an analogous process accompanying in their formation or alteration.

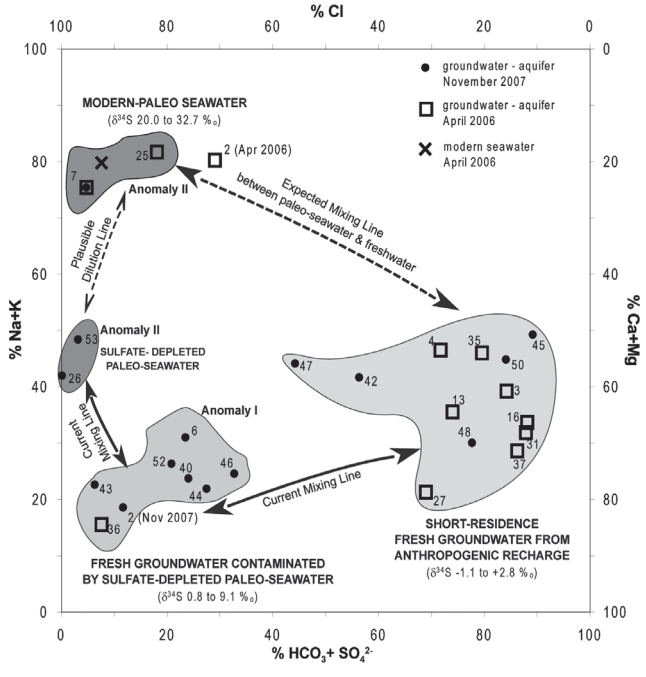

Figure 7. Chebotarev diagram showing the percentages of Na+K, Cl, HCO_3+SO_4 and Ca+Mg in groundwater from the Costa de Hermosillo aquifer. The measurements for April of 2006 were adopted from Szynkiewicz et al. (2008)

Rise of seawater level due to climate fluctuations and tectonic activity may cause a temporary change of environmental condition in coastal areas and involve a development of marine settings with salty and brackish waters. Once buried in sediments this saline water may be stored for a long period of time within the aquifers and act as an important source of salinization (e.g., Klein-BenDavid et al. 2004; Rosenthal et al. 2006). For instance, salinization caused by mobilization of traces of paleo-sea wedge due to overpumping of aquifer has been proposed

for the coastal aquifer of the Gulf of Guinea (Akouvi et al. 2008). In the Costa de Hermosillo aquifer, at least one sea transgression occurred in the past and caused inland sedimentation of blue clays with marine fauna during the Miocene (Monreal et al. 2000). Today, these clays reside on different depths, typically 100 to 200 m beneath the western portion of the upper aquifer (Rangel-Medina 2006). The spatial distribution of the blue clays likely overlaps with the locations of saline anomalies, thus, they appear to be the most plausible source of paleo-seawater. Szynkiewicz et al. (2008) reported a significant alteration of the paleo-seawater for Well 7 (at depth of –30 m) which was manifested by sulfate depletion (~147 mg/L) likely resulted from microbial sulfate reduction in the past. In November of 2007, more detailed, vertical analyses on Well 7 provided a new evidence for an existence of unaltered seawater at deeper depths of II Anomaly (Figure 4, 7; Table 2). In contrast to the water table of Well 7, at depths of –40 and –67 m the groundwater showed high ratios of SO_4/Cl and Cl/Br (0.09 to 0.10 and 268 to 294, respectively), high $d^{18}O$-d^2H values (–1.4 to –1.0 ‰ and –18 to –17 ‰, respectively) and high $d^{34}S$ values (+20 to +23.2 ‰) which were similar to the seawater of the Gulf of California (SO_4/Cl = 0.11 to 0.14; Cl/Br = 256 to 266; $d^{18}O$-d^2H values = 0.3 to 0.6 and –6 to –5 ‰, respectively; $d^{34}S$ = +20.4 to +20.6 ‰; after Szynkiewicz et al. 2008).

In contrast to Well 7, two other abandoned wells from II Anomaly (no. 26 and 53) showed distinctively lower $d^{18}O$-d^2H values and lower salt content (Table 2). Whereas lower mineralization of water may result from a variety of local factors (e.g., variation in the abundance of crystalline rocks versus evaporites in the bedrock, different rates of dilution by subsequent recharge), the $d^{18}O$-d^2H values are more sensitive indicators of water origin because seawater shows a consistent value of ~0 ‰ for $d^{18}O$ and d^2H compared to more negative values of $d^{18}O$-d^2H for meteoric precipitation in the continents (e.g., Sharp 2006). Currently, typical rainfall in the Costa de Hermosillo aquifer ranges from –7.6 to –3.8 ‰ for $d^{18}O$ value and from –55 to –36 ‰ for d^2H value (Szynkiewicz et al. 2008). These ranges overlap with the isotope compositions noted for Wells 26 and 53, –6.1 to –4.4 ‰ for $d^{18}O$ values and –45 to –33 ‰ for d^2H values (Figure 8), and strongly indicate for a substantial contribution of fresh groundwater originated from the inland rainfall.

The stratigraphy of the Costa de Hermosillo aquifer is based on only three deep boreholes. This, in turn, makes it difficult to define where in the sedimentary section a given saline intrusion was originally derived. The Costa de Hermosillo aquifer, however, resides in the sedimentary graben formed during tectonic extension and rift evolution related to opening of the Gulf of California (Csérna de 1989; Monreal et al. 2000). Recent studies on rift valleys show that brines of varying salinity and chemical composition might be isolated at different stages in their evolution as a result of tectonic evolution of the rift system. The development of the rift system appears to control the evolution of distinctive paleoenvironments such as marine lagoons and terminal lakes (e.g., Klein-Ben et al. 2004; Rosenthal

et al. 2006) which, over time, may develop distinctive hydrological settings with highly saline groundwater. Therefore, it might be suggested that saline groundwater with negative $d^{18}O$-$d^{2}H$ values, observed for Wells 26 and 53 (Figure 8), could have been developed in another coastal environment formed after the Miocene/Pliocene sea transgression. This might have been a setting of terminate lake which was more dominated by the surface run-off and the groundwater recharge originated from the meteoric precipitation in the nearby highlands of the Sierra Madre Mountains.

Alternatively, the saline groundwater with lower $d^{18}O$-$d^{2}H$ values may have originated from the same paleo-seawater, such as in Well 7, but it could have been partly flashed out by meteoric water in a subsequent process. For instance, an essential dilution of basinal brines of Miocene age by freshwater was reported for the Jordan-Dead Sea Rift Valley (e.g., Vengosh et al. 1994b; Bergelson et al. 1999; Rosenthal et al. 2006). In Figure 8, a possible dilution line is inferred from a positive correlation between $d^{18}O$ and $d^{2}H$ values ($R^2 = 0.98$) which parallels the Sonoran Meteoric Water Line that defines a typical, kinetic fractionation for hydrogen and oxygen isotopes in the Costa the Hermosillo aquifer. The occurrence of dilution is also supported by lower values of electric conductivity for Wells 26 and 53 (3.2 to 26.4 mS/cm) compared to Well 7 (17.9 to 41.7 mS/cm). Although dilution by meteoric water decreases concentrations of ions and causes a negative excursion of $d^{18}O$-$d^{2}H$ values, it does not change proportions of particular ions dissolved in water. In particular, chloride and bromide are good paleo-tracers because of their small concentrations in precipitation, high solubility in water and conservative behavior when ionized in water (e.g., Davis et al. 1998). For Wells 26 and 53, the Cl/Br ratios varied in similar range, 309 to 361 (Table 3), such as at the bottom of Well 7 (ratios 268 to 294, Table 3) and modern seawater (256 to 266, after Szynkiewicz et al. 2008), thus, suggest a similar marine origin for all contaminated wells (no. 7, 26, 53) detected in II Anomaly.

Table 4. Vertical variations of bromide and chloride concentrations for groundwater samples taken from abandoned wells (II Anomaly) in November of 2007. b.d. – below detection.

Well No.	Well Name	Depth [m]	Br [mg/L]	Cl [mg/L]	Cl/Br
7	Campo Dec	-30	390	10649	27
		-40	221	64976	294
		-67	252	67779	268
26	MD-05	-31	133	41146	309
		-41	133	44176	332
		-61	130	46949	361
53	Campo Cuatro 2	-34	b.d.	1037	b.d.
		-44	b.d.	1542	b.d.
		-53	11	3497	317

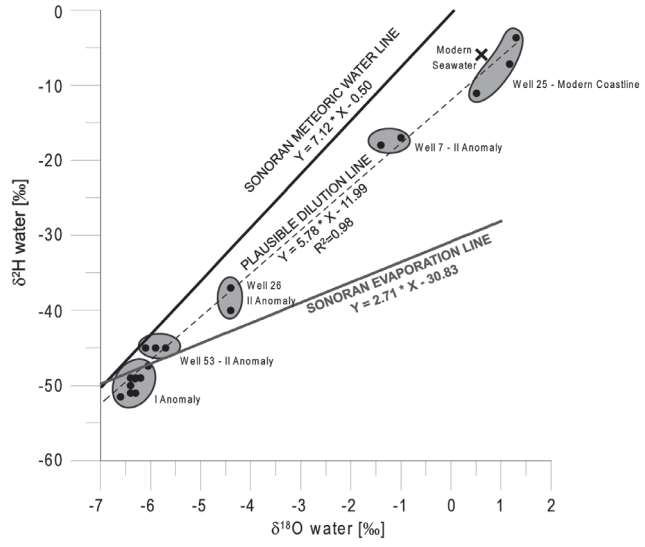

Figure 8. Variations of δ^2H and $\delta^{18}O$ values of groundwater (November of 2007) in I and II Anomaly relative to the Sonoran Meteoric Water Line and the Sonoran Evaporation Line calculated by Szynkiewicz et al. (2008). The δ^2H and $\delta^{18}O$ values of modern seawater and Well 25 (a contaminated offshore well) were adopted from Szynkiewicz et al. (2008)

A relatively small concentration of sulfate in the upper portion of paleo-seawater (148 mg/L for the groundwater table of Well 7) and the absence of sulfate (<1 mg/L) in the saline groundwater of Wells 26 and 53 are the most striking phenomena that distinguishes these saline intrusions from the modern seawater which is characterized by high sulfate concentrations (2,552 to 3,961 mg/L; after Szynkiewicz et al. 2008). Similar sulfate depletion in seawater intrusions (down to 1 mg/L) was observed in several wells of southern Italy located ~1.5 km inland from the coast (Capaccioni et al. 2005).

Based on abnormally high $\delta^{34}S$ values of +32 ‰ for sulfate in Well 7 and small SO_4/Cl and Cl/Br ratios of 0.01 and 33, respectively, Szynkiewicz et al. (2008) inferred the advanced alteration of paleo-seawater resulted from microbial sulfate reduction. In anoxic seawater and marine sediment porewater, microbial sulfate reduction is mainly responsible for the decrease of sulfate concentrations, the increase of $\delta^{34}S$ values of sulfate (e.g., Canfield 2001; Brüchert 2004), the increase of bromide concentrations (Long and Gudramovics 1983), and lowering of Cl/Br ratio. Similarly as in previous seasons (Szynkiewicz et al. 2008), in this study the $\delta^{34}S$ value was same high, +32.4 ‰, at the water table (–30 m) of Well 7 but it had distinctively lower values compared to the groundwater at lower depths of this well, +23.2 ‰ at depth of -40 m and +20.0 ‰ at depth of –67 m. The lower $\delta^{34}S$ values were similar to the seawater implying a small extent of alteration by sulfate reduction. This likely indicates that microbial sulfate reduction was restricted to a relatively narrow zone of the sediments in the past. In contrast to Well 7, the saline groundwater from Wells 26 and 53 had sulfate of < 1 mg/L

along the entire water columns of ~30 m long (Table 2) which strongly suggests a complete removal of sulfate ions by microbial sulfate reduction. Generally, in marine sediments microbial sulfate reduction is restricted to the upper portions of sediments and the increase of sulfate concentrations has been observed with increasing depth (e.g., Albert et al. 1995; Reeburgh et al. 2006). Given that saline groundwater within II Anomaly showed different patterns of sulfate depletion (<1 mg/L to 3,961 mg/L), it is speculated that salinization of these wells most likely resulted from the intrusions of isolated portions of the paleo-seawater from different depths of marine strata underlying the upper aquifer of the Costa de Hermosillo aquifer.

5.2. Age of paleo-seawater — strontium isotopes

Strontium isotope data provide some additional constraints on the possible age and modes of origin of groundwater in the Costa de Hermosillo aquifer (Figure 6, Table 4). Most importantly, the measured $^{87}Sr/^{86}Sr$ ratio of strontium in the groundwater sampled from Well 25 (0.709181), located ~300 m from the coastline, is identical to that of modern seawater (~0.709175; McArthur et al. 2001) and so confirms the conclusion that this well has been contaminated by present-day seawater (Szynkiewicz et al. 2008). Groundwater in Well 7, in contrast, has been interpreted as Mio-Pliocene seawater originally trapped in sediments deposited during a Miocene marine transgression (Szynkiewicz et al. 2008). However, the strontium isotope composition of the groundwater in Well 7 (0.70833) is too low to represent strontium from seawater of this age (Figure 6). Instead, the strontium isotopic composition of Well 7 water overlaps the values for early Miocene seawater (20–23 Ma). This age is considerably older than any estimate of the timing of early extensional tectonism and marine transgression ultimately associated with the opening of the Gulf of California, which is considered to be Mio-Pliocene in age (~ 4–6 Ma) at the latitude of Tiburón Island (Figure 1) (Oskin and Stock 2003). Given the lack of geologic evidence for an early Miocene marine transgression in west-central Sonora, it seems unlikely that the groundwater of Well 7 contains strontium from trapped early Miocene age seawater. Assuming that other chemical characteristics of the Well 7 water require that it ultimately represents seawater, then the strontium isotopic composition of this water must have been modified since trapping. Prolonged interaction between Mio-Pliocene seawater ($^{87}Sr/^{86}Sr$ ~ 0.709002; Figure 6) and surrounding sedimentary material is the most likely mechanism for producing such modification (Johnson and DePaolo 1994). For example, if the Well 7 water represents the product of interaction between trapped Mio-Pliocene seawater and sediments derived predominately from the local, Late Cretaceous granitic rocks of the Coastal Sonora Batholith (measured $^{87}Sr/^{86}Sr$ ~ 0.7067 and 0.7076; Valencia-Moreno et al. 2003), then the Well 7 water would have to contain ~40%

sediment-derived strontium. However, it is important to note that the strontium isotopic composition of the Well 7 groundwater alone does not actually provide any firm constraints on the origin of this water. The Well 7 water, surface evaporated meteoric waters (Wells 26, 53), "fresh" anthropogenic recharge (Wells 31, 3), and modern surface water from the Hermosillo Dam, all have similar strontium isotope compositions, regardless of their strontium contents (Figure 6). This indicates that in the inland portions of the Costa de Hermosillo aquifer, strontium isotopic data cannot discriminate between the various ground and surface waters that we have identified in this region. All we can state with certainty on the basis of the strontium isotopic data alone is that saline groundwaters from these inland regions do not represent incursions of modern seawater from the Gulf of California.

5.3. Shape of paleo-seawater intrusions

Defining a shape of modern- and paleo-seawater intrusions is difficult because most of the exploratory wells in coastal aquifers are shallow and do not reach a saline/freshwater interface. The gravimetric and numerical models imply that deeper-seated saline waters typically occur as the saline/seawater wedges (e.g., Post et al. 2003; Giambastiani et al. 2007; Duque et al. 2008) in the low-permeability lenses of confined aquifers (Akouvi et al. 2008).

In this study, the paleo-seawater intrusions of II Anomaly appear to reside at the depths of current water table (–34 to –30 m) and continue down to the bottom of the abandoned wells (–67 to –53 m) as inferred from the high values of electric conductivity and the distinctive chemical and isotope compositions in vertical scale for Wells 7, 26 and 53 (Table 2). Currently, no deep bore holes exist in this part of the Costa de Hermosillo aquifer which would allow for accurate evaluations on the extent of paleo-seawater with depth. Some farmers, however, were successful in drilling through the contaminated portion of the aquifer and reached the levels of fresh groundwater which likely underlies the paleo-seawater of II Anomaly. For example, Well 6, which is situated in a distance of 500 m from the contaminated Well 53 in II Anomaly (Figure 1A), has been effectively used for irrigation because it was cased with the concrete at lower depths in which the paleo-seawater was present. Currently, Well 6 pumps water from depths of ~350 to 400 m and extract water from the lower aquifer. This observation supports the hypothesis that under current condition the lenses of paleo-seawater reside near the water table of the upper aquifer of the Costa the Hermosillo.

One would expect that over time a dense water of paleo-seawater intrusions should sink into the underlying freshwater of lower density; however, their current position near the water table suggest that they might be isolated from lower depths by low-permeability layers of confined sediments. Historical reports indicate that salinization in II Anomaly occurred relatively fast, during first 10–15

years of agricultural operation (after Miller 1994; Halvorson et al. 2003). Because this area is faulted due to tectonic extension (Csérna 1989; Rangel-Medina et al. 2004), it is likely that a rapid migration of paleo-seawater could have occurred along the tectonic fractures, thus, at present time the paleo-seawater might be separated from the source layers of the blue clays by other low-permeable sediments of the upper aquifer. Alternatively, the blue clay strata may be present at shallower depths in this portion of the aquifer and act as a barrier which prevents from the returning recharge because of the lower permeability of clays. On Figure 10, a simplified model is presented which shows the plausible position and shape of the paleo-seawater within II Anomaly as inferred from the presented chemical and isotope data set.

Lack of a good management plan has led to the casing of new extraction wells with the concrete at depths with paleo-seawater. Apparently, this brings a temporary solution. It is likely that, over time, the slow recharge of paleo-seawater through the less-permeable clay strata may lead to the contamination of fresh groundwater at bigger depths of the lower aquifer. A beginning of this process has been inferred from Well 6 (II Anomaly), which showed elevated chloride concentrations (339 mg/L) and higher $\delta^{34}S$ values (9.1 ‰) indicative for a partial mixing with paleo-seawater (Figure 7). Based on chemical and isotope compositions alone, however, it is impossible to evaluate whether the mixing results from 1) the upconing of new portions of paleo-seawater which might still reside at bigger depths, or 2) from the recharge of the already intruded paleo-seawater detected in Well 53 that currently resides near the water table. It is likely that both processes may gain importance and may involve a prolonged contamination of new extraction wells.

5.4. Origin of salinity in I Anomaly

A beginning of salinization has been observed for I Anomaly (Steinich et al. 1998) which is located ~25 km northward from II Anomaly already contaminated by paleo-seawater (Figure 1). On the Chebotarev diagram, groundwater from I Anomaly is situated below the sulfate-depleted paleo-seawater detected in II Anomaly (Figure 7). This likely suggests a prevailing, current mixing between fresh groundwater and sulfate-depleted paleo-seawater. Because of sulfate-poor reservoir in the paleo-seawater, the I Anomaly appeared to be spatially unrecognizable based on sulfate concentrations (Figure 3), but it was clearly outlined by a concentric pattern of increasing values of chloride concentrations (Figure 2). This confirms a similar origin of saline groundwater such as in II Anomaly.

Although the sulfate-depleted paleo-seawater detected in II Anomaly had sulfate <1 mg/L (Table 2), the concentric pattern of increasing values of $\delta^{34}S$ values within I Anomaly (Figure 7) indicates a possible mixing with the paleo-seawater less altered by sulfate reduction. In particular, Well 2 appeared to be the most af-

fected by this process and revealed significant, seasonal changes in chemical and isotope compositions over time. Along the sampling campaigns in 2005 and 2006, Well 2 showed considerable changes in concentrations of sulfate (90 to 632 mg/L), chloride (922 to 1287 mg/L) and large variation of $\delta^{34}S$ values (5.6 to 8.2 ‰) (Szynkiewicz et al. 2008). During the 2006 campaign this well was situated next to the field of unaltered seawater on the Chebotarev diagram (Figure 7) which may suggest a bigger contribution of unaltered paleo-seawater by microbial sulfate reduction compared to November 2007 (this study) in which Well 2 was placed in the field of I Anomaly implying larger contribution of sulfate-depleted paleo-seawater (Figure 7).

In the Costa de Hermosillo, the recharge of surface water from excess irrigation was recorded by elevated contents of nitrate compounds (Steinich et al. 1998; Szynkiewicz et al. 2008) and elevated contents of sulfate. On the Chebotarev diagram (Figure 7), the anthropogenic recharge is inferred from increasing proportions of sulfate, bicarbonate, sodium and potassium; this is caused by the anthropogenic enrichment of the irrigated water in sulfate ions from sulfate-rich fertilizers and evaporation of irrigation water (Szynkiewicz et al. 2008). Because the anthropogenic sulfate is characterized by distinctive lower $\delta^{34}S$ values, –2 to +3 ‰ (Szynkiewicz et al. 2008) compared to the higher $\delta^{34}S$ values of sulfate from paleo-seawater, an essential mixing between groundwater from I Anomaly and anthropogenic recharge was also recorded by the increase of sulfate concentration relative to the decrease of $\delta^{34}S$ values (R = –0.81; Figure 9) and by the increase of chloride concentration relative to the increase of $\delta^{34}S$ values (R = 0.78; Figure 9). It is likely that modern anthropogenic recharge may temporary prevent from further contamination of the upper aquifer by sulfate-depleted paleo-seawater and/or causes a significant dilution of paleo-seawater in this part of the aquifer.

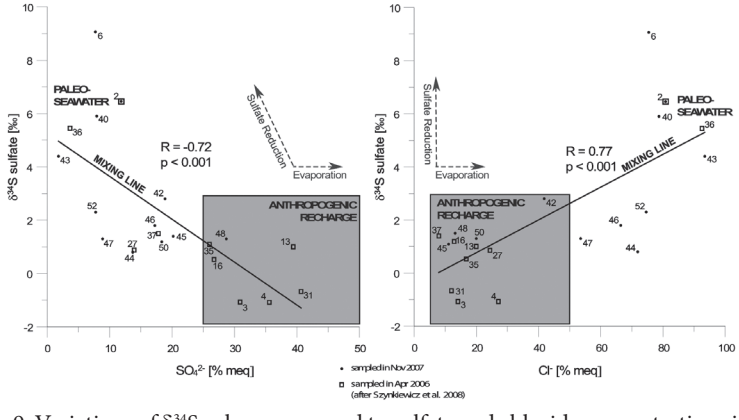

Figure 9. Variations of $\delta^{34}S$ values compared to sulfate and chloride concentrations in the Costa de Hermosillo Aquifer. The range of $\delta^{34}S$ of sulfate for anthropogenic recharge (grey field) is cited after Szynkiewicz et al. (2008). The trends of expected changes of $\delta^{34}S$ due to evaporation and microbial sulfate reduction are shown and compared to the mixing line of two end member waters (anthropogenic recharge and paleo-seawater)

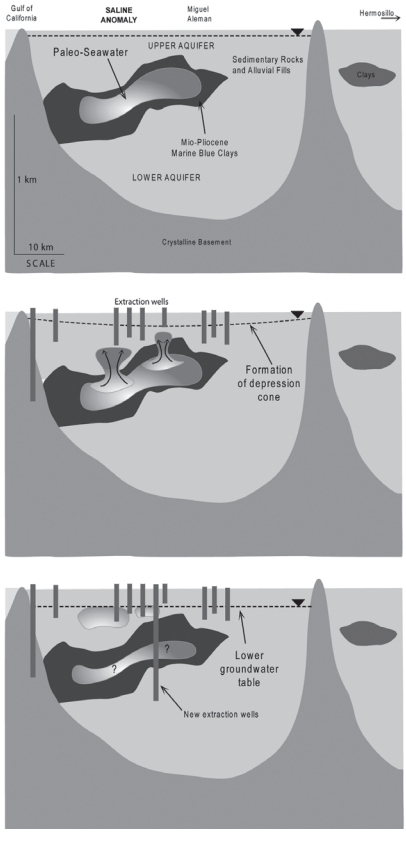

Figure 10. Simplified theoretical model showing general processes causing contamination of the Costa de Hermosillo in II Anomaly due to upward migration of the paleo-seawater from the upper portion of the blue clay strata

During sampling in the area of I Anomaly, two wells were found for which the pumping devices were removed ("CW" symbol on Figure 1A) similarly as for the abandoned wells of II Anomaly. Those wells had no access in the time of sampling in November of 2007, however, they appear to be excluded from agricultural activity because of elevated salt content which was too high to support agricultural activity. This implies that small lenses of paleo-seawater may be already present at the water table of I Anomaly. Nevertheless, the groundwater in I Anomaly shows smaller extent of contamination by paleo-seawater intrusion compared to II Anomaly which indicates a large chemical heterogeneity of paleo-seawater trapped within the aquifer, most likely due to different dilution by the subsequent freshwater recharge (Figure 10).

Overall, the local character and the distinctive, spatial geochemical variations of the paleo-seawater in the Costa de Hermosillo aquifer suggest that paleo-seawater intrusions most likely originated from the isolated lenses of paleo-seawater which have not been flashed out by the subsequent freshwater recharge since the Mio-Pliocene transgression. The geometry of this aquifer was largely controlled by

the extensive faulting and basin subsidence, related to the opening of the Gulf of California, in the past. It is likely that tectonic subsidence might have led to formation of subbasins with varied sediment thickness which isolated various portions of the marine sediments with the Mio-Pliocene paleo-seawater and prevented from flashing out by subsequent freshwater recharge from the nearby highlands of the Sierra Madre Mountains. Therefore, tectonism appears to be an important factor leading to preservation of seawater from former sea transgressions in the coastal rift valleys.

6. Conclusions

This study shows a distinctive evidence for irreversible changes in water quality resulted from the paleo-seawater intrusions which have occurred in a large distance of ~20–32 km from the modern coastline of the Gulf of California because of extraction of fresh groundwater for agricultural operation. In the most contaminated portion of this aquifer (II Anomaly), the paleo-seawater intrusions presently occur in the form of saline lenses that reside at the current groundwater table (~ –30 meters). The spatial geochemical variability of intrusions and their local character suggest that they originated from the isolated portions of paleo-seawater which overtime underwent incomplete dilution by the subsequent recharge of fresh groundwater from the highlands of Sierra Madre. Tectonic subsidence during the opening of the Gulf of California was likely the major factor leading to the isolations of some portions of the paleo-seawater within the aquifer and the inhomogeneous flashing out of this paleo-seawater in the past.

Strontium isotopes did not allow for a proper discrimination on the age of paleo-seawater because of the prolonged groundwater-rock interaction which led to the lowering of the $^{87}Sr/^{86}Sr$ ratio as a result of strontium isotope exchange between groundwater and crystalline basement. Nevertheless, strontium isotopes appear to be useful tool for recognizing the modern front of seawater intrusion in the offshore areas of the Gulf of California. Based on spatial, stratigraphic and geochemical relationships observed for the studied paleo-seawater intrusions and the stratigraphic position of the marine blue clay strata, it is indirectly inferred that extensive salinization of the Costa de Hermosillo aquifer most likely resulted from the intrusion of Mio-Pliocene seawater trapped in the aquifer's sediments during tectonic evolution of the studied area (Table 10).

The formation of I Anomaly apparently results from the incursion of the sulfate-depleted paleo-seawater of similar origin such as observed for II Anomaly. The modern anthropogenic recharge appears to temporary prevent from further contamination of the upper aquifer by sulfate-depleted paleo-seawater. It is also likely that the paleo-seawater residing under I Anomaly is more diluted compared to II Anomaly, which, in turn, involves a smaller salinization of fresh groundwater in the central Costa de Hermosillo aquifer.

Acknowledgments

This study was supported by grants from the Stable Isotope Research Facility in the Indiana Laboratory in Bloomington under the supervision of L. Pratt and E. Ripley, and from the Universidad de Sonora in Hermosillo, Mexico. We gratefully acknowledge technical assistance from Peter Sauer, Adam Johnson, Ericka Elswick, Craig Moore and Steve Studley.

References

Akouvi, A., M. Dray, S. Violette, G. de Marsilu, G.M. Zuppi. 2008. The sedimentary coastal basin of Togo: Example of a multilayered aquifer still influenced by paleo-seawater intrusion. *Hydrogeology Journal*, 16, pp. 419–436.

Albert, D.B., C. Taylor, C.S. Martens. 1995. Sulfate reduction rates and low molecular weight fatty acid concentrations in the water-column and surficial sediments of the Black Sea. *Seep-Sea Research*, 42, pp. 1239–1260.

Arakel, A.V., W.F. Ridley. 1986. Origin and geochemical evolution of saline groundwater in the Brisbane coastal plain, Australia. *Catena*, 13, pp. 257–275.

Bergelson, G., R. Nativ, A. Bein. 1999. Salinization and dilution history of ground water discharging into the Sea of Galilee, the Dead sea Transform, Israel. *Applied Geochemistry*, 14, pp. 91–118.

Bond, L.D., J.D. Bredehoeft. 1987. Origins of seawater intrusion in a coastal aquifer — a case study of the Pajaro Valley, California. *Journal of Hydrology*, 92, pp. 363–388.

Brand W.A., H. Avak, R. Seedorf, D. Hofmann, T. Conradi. 1996. New methods for fully automated isotope ratio determination from hydrogen at the natural abundance level. *Isotopes in Environmental and Health Studies*, 32, pp. 263–273.

Brüchert, V. 2004. Physiological and ecological aspects of sulfur isotope fractionation during bacterial sulfate reduction. In: J.P. Amend, K.J. Edwards, T.W. Lyons (eds.), *Sulfur Biogeochemistry. Special Paper*, vol. 379. Geological Society of America, Boulder.

Canfield, D.E. 2001. Biogeochemistry of sulfur isotopes. In: J.W. Valley, D.R. Cole (eds.) *Stable Isotope Geochemistry*. Mineralogical Society of America, Blacksburg, VA, vol. 43, pp. 607–636.

Capaccioni, B., M. Didero, C. Paletta, L. Didero. 2005. Saline intrusion and refreshening in a multilayer coastal aquifer in the Catania Plain (Sicily, Southern Italy): Dynamics of degradation processes according to the hydrochemical characteristics of groundwaters. *Journal of Hydrology*, 307, pp. 1–16.

Conti, A., E. Sacchi, M. Chiarle, G. Martinelli, G.M. Zuppi. 2000. Geochemistry of the formation waters in the Po plain (Northern Italy): An overview. *Applied Geochemistry*, 15, pp. 51–65.

Criss, R.E., M.L. Davisson. 1996. Isotopic imaging of surface water/groundwater interactions, Sacramento Valley, California. *Journal of Hydrology*, 178, pp. 205–222.

Csérna, Z. de 1989. An outline of the geology of Mexico. In: A.W. Bally, A.R. Palmer (eds.) *The Geology of North America, An overview*. Boulder Colorado, Geol.Soc.of Am., pp. 233–264.

Custodio, E. 2010. Coastal aquifers of Europe: An overview. *Hydrogeology Journal*, 18, pp. 269–280.

Daesslé, L.W., E.C. Sánchez, V.F. Camacho-Ibar, L.G. Mendoza-Espinoza, J.D. Carriquiry, V.A. Macias, P.G. Castro. 2004. Geochemical evolution of groundwater in the Maneadero coastal aquifer during a dry year in Baja California, Mexico. *Hydrogeology Journal*, 13, pp. 584–595.

Davis, S.N., D.O. Whittemore, J. Fabryka-Martin. 1998. Uses of chloride/bromide ratios in studies of potable water. *Groundwater*, 36, pp. 338–350.

Demirel, Z. 2004. The history and evaluation of saltwater intrusion into a coastal aquifer in Mersin, Turkey. *Journal of Environmental Management*, 70, pp. 275–282.

Duque, C., M.L. Calvache, A. Pedrera, W. Martin-Rosales, M. López-Chicano. 2008. Combined time domain electromagnetic soundings and gravimetry to determine marine intrusion in a detrital coastal aquifer (Southern Spain). *Journal of Hydrology*, 349, pp. 536–547.

Fass, T., P.G. Cook, T. Stieglitz, A.L. Herczeg. 2007. Development of saline ground water through transpiration of sea water. *Ground Water*, 45, pp. 703–710.

Faye, S., S.C. Faye, S. Ndoye, A. Faye. 2003. Hydrogeochemistry of the Saloum (Senegal) superficial coastal aquifer. *Environmental Geology*, 44, pp. 127–136.

Ghabayen, S.M.S., M. McKee, M. Kemblowski. 2006. Ionic and isotopic ratios for identification of salinity sources and missing data in the Gaza aquifer. *Journal of Hydrology*, 318, pp. 360–373.

Giambastiani, B.M.S., M. Antonellini, G.H.P. Oude Essink, W.J. Stuurman. 2007. Saltwater intrusion in the unconfined coastal aquifer of Ravenna (Italy): A numerical model. *Journal of Hydrology*, 340, pp. 91–104.

Giménez-Forcada E. 2014. Space/time development of seawater intrusion: A study case in Vinaroz coastal plain (Eastern Spain) using HFE-Diagram, and spatial distribution of hydrochemical facies. *Journal of Hydrology*, available online.

Giménez, E., I. Morell. 1997. Hydrogeochemical analysis of saliznization processes in the coastal aquifer of Oropesa (Castellón, Spain). *Environmental Geology*, 29, pp. 118–131.

Grass, S., H.H.G. Savenije. 2008. Salt intrusion in the Pungue estuary, Mozambique: Effect of sand banks as a natural temporary salt intrusion barrier. *Hydrology and Earth System Sciences Discussions*, 5, pp. 2523–2542.

Han D., C. Kohfahl, X. Song, G. Xiao, J. Yang. 2011. Geochemical and isotopic evidence for palaeo-seawater intrusion into the south coast aquifer of Laizhou Bay, China. *Applied Geochemistry*, 26, pp. 863–883.

Halvorson, W.L., A.E. Castellanos, J. Murrieta-Saldivar. 2003. Sustainable land use requires attention to ecological signals. *Environmental Management*, 32, pp. 551–558.

Horita J., A. Ueda, K. Mizukami, I. Takatori. 1989. Automatic δD and $\delta^{18}O$ analyses of multi-water samples using H_2- and CO_2-water equilibration methods with a common equilibration set-up. *Applied Radiation and Isotopes*, 40, pp. 801–805.

Hussein, M.T. 1982. Evaluation of groundwater resources in Tokar Delta, Sudan. *Hydrological Sciences Journal*, 27, pp. 139–145.

Johnson, T.M., D.J. DePaolo. 1994. Interpretation of isotopic data in groundwater-rock systems — model development and application to Sr isotope data from Yucca Mountain. *Water Resources Research*, 30(5), pp. 1571–1587.

Jones, B.F., A. Vengosh, E. Rosenthal, Y. Yechieli. 1999. Geochemical Investigations. In: J. Bear et al. (eds.) *Seawater Intrusion in Coastal Aquifers — Concepts, Methods and Practices*. Kluwer Academic Publishers, (np), pp. 51–71.

Kim, Y., K.-S. Lee, D.-C. Koh, D.-H. Lee, S.-G. Lee, W.-B. Park, G.-W. Koh, N.-C. Woo. 2003a. Hydrogeochemical and isotopic evidence of groundwater salinization in a coastal aquifer: A case study in Jeju volcanic island, Korea. *Journal of Hydrology*, 270, pp. 282–294.

Kim, J.H., R.H. Kim, J. Lee, H.W. Chang. 2003b. Hydrogeochemical characterization of major factors affecting the quality of shallow groundwater in the coastal area at Kimje in South Korea. *Environmental Geology*, 44, pp. 478–489.

Klein-Ben, O.D., E. Sass, A. Katz. 2004. The evolution of marine evaporatic brines in inland basins: The Jordan-Dead Sea Rift valley. *Geochimica et Cosmochimica Acta*, 68, pp. 1763–1755.

Kohout F.A. 1960. Cyclic flow of salt water in the Biscayne aquifer of Southeastern Florida. *Journal of Geophysical Research*, 65, pp. 2133–2141.

Konikow, L.F., T.E. Reilly. 1999. Seawater intrusions in United States. In: J. Bear et al. (eds.) *Seawater Intrusion in Coastal Aquifers — Concepts, Methods and Practices*. Kluwer Academic Publishers, (np), pp. 463–506.

Long, D.T., R. Gudramovics. 1983. Major-element geochemistry of brines from the Wind Tidal Flat area, Laguna Madre, Texas. *Journal of Sedimentology and Petrology*, 53, pp. 797–810.

Lee, J.-Y., S.H. Song. 2007. Evaluation of groundwater quality in coastal areas: Implications for sustainable agriculture. *Environmental Geology*, 52, pp. 1231–1242.

Ma, F., Y.S. Yang, R. Yuan, Z. Cai, S. Pan. 2006. Study of shallow groundwater quality evolution Ander saline intrusion with environmental isotopes and geochemistry. *Environmental Geology*, 51, pp. 1009–1017.

Magaritz, M., J.E. Luzier. 1985. Water-rock interactions and seawater-freshwater mixing effects in the coastal dunes aquifer, Coos Bay, Oregon. *Geochimica et Cosmochimica Acta*, 49, pp. 2515–2525.

Martínez, D.E., E.M. Bocanegra. 2002. Hydrogeochemistry and cation-exchange processes in the coastal aquifer of Mar Del Plata, Argentina. *Hydrogeology Journal*, 10, pp. 393–408.

McArthur, J.M., R.J. Howarth, T.R. Bailey. 2001. Strontium isotope stratigraphy: LOWESS version 3: Best fit to the marine Sr-isotope curve for 0-509 Ma and accompanying look-up table for deriving numerical age: *Journal of Geology*, 109, pp. 155–170.

Melloul, A.J., D.G. Zeitoun. 1999. A semi-empirical approach to intrusion monitoring in Israeli coastal aquifer. In: J. Bear et al. (eds.) *Seawater Intrusion in Coastal Aquifers — Concepts, Methods and Practices*. Kluwer Academic Publishers, (np), pp. 543–558.

Mercado, A. 1985. The use of hydrogeochemical patterns in carbonate dand and sandstone aquifers to identify intrusion and flushing of saline water. *Ground Water*, 23, pp. 635–645.

Miller, G.T. Jr. 1994. *Living in the Environment: Principles, Connections, and Solutions*. Wadsworth Publishing, Belmont, California.

Monreal, R., J. Castillo, M. Rangel, M. Morales. 2000. Estudio geohidrológico del comportamiento del acuífero mediante la realización de pruebas de bombeo y conceptualización a detalle de la intrusión salina en el acuífero de la Costa de Hermosillo #65533; Informe Final de Proyecto en colaboración con la Comisión Nacional del Agua- Universidad de Sonora. Febrero a Agosto de 2000 (in Spanish).

Nadler, A., M. Magaritz, E. Mazor. 1980. Chemical reactions of seawater with rocks and freshwater: Experimental and field observations on brackish waters in Israel. *Geochimica at Cosmichimica Acta*, 44, pp. 879–886.

Oskin, M., J. Stock. 2003. Marine incursion synchronous with plate-boundary localization in the Gulf of California. *Geology*, 31, pp. 23–26.

Panagopoulos, G., N. Lambrakis, P. Tsolis-Katagas, D. Papoulis. 2004. Cation exchange processes and human activities in unconfined aquifers. *Environmental Geology*, 46, pp. 542–552.

Petalas C., N. Lambrakis. 2006. Simulation of intense salinization phenomena in coastal aquifers — the case of the coastal aquifers of Thrace. *Journal of Hydrology*, 324, pp. 51–64.

Post, V.E.A., H. Van der Plicht, H.A.J. Meijer. 2003. The origin of brackish and saline groundwater in the coastal area of the Netherlands. *Netherlands Journal of Geosciences (Geologie en Mijnbouw)*, 82, pp. 133–147.

Rangel-Medina, M. 2006. Propuesta de un modelo integral para la recuperación de acuífero intrusionado, sometido a uso intensivo de aqua subterránea: el acuífero costa de Hermosillo, Sonora, México. [Ph. D. Thesis] Biblioteca del Instituto de Geofisica, Universidad Nacional Autónoma de México (in Spanish).

Rangel-Medina, M., S.R. Monreal, M.M. Morales, J. Castillo Gurrola. 2004. Estimation of the vulnerability to saline intrusion of the coast of Hermosillo aquifer, Sonora, Mexico. *Geofísica International*, 43, pp. 611–621.

Rangel-Medina, M., R. Monreal, M. Morales, J. Castillo. 2003. Caracterización gequímica e isotópica del aqua subterránea y determinación de la migarción marina en el acuífero de la Costa de Hermosillo, Son, México. Publicaciones del Instituto Geológico y Minero de España, Serie Hidrogeología y aguas subterráneas 8, pp. 325–335. Tomo I.

Rangel-Medina, M., R. Monreal, M. Morales, J. Castillo. 2002. *Determinación de la vulnerabilidad a la intrusión marina de acuíferos costeros en el pacifico norte mexicano; un caso, el acuífero costa de Hermosillo Sonora, México*. Página web del CYTED XVII <http://www.tierra.rediris.es/hdrored/ponecias/Rangel.html>.

Reeburgh, W.S., S.C. Tyler, J. Carroll. 2006. Stable carbon and hydrogen isotope measurements on Black Sea Water-column methane. *Deep-Sea Research*, 53, pp. 1893–1900.

Rosenthal, E., A. Akiva, P. Möller. 2006. The paleoenvironmental and the evolution of brines in the Jordan-Dead Sea transform and in adjoining area. *International Journal of Earth Sciences*, 95, pp. 725–740.

Sadeg, S.A., N. Karahanoğlu.. 2001. Numerical assessment of seawater intrusion in the Tripoli region, Libya. *Environmental Geology*, 40, pp. 1151–1168.

Schmorak, S. 1967. *Salt water encroachment in the coastal plain of Israel*. IASH, Haifa Symposium.

Sivan, O., Y. Yechieli, B. Herut, B. Lazar. 2005. Geochemical evolution and timescale of seawater intrusion into the coastal aquifer of Israel. *Geochimica et Cosmochimica Acta*, 69, pp. 579–592.

Sharp, Z. 2006. *Principles of Stable Isotope Geochemistry*. Prentice Hall, A. miejsce wydania?

Sherif, M.M., V.P. Singh, A.M. Amer. 1990. A note on saltwater intrusion in coastal aquifers. *Water Resources Management*, 4, pp. 123–134.

Steinich, B., O. Escolero, L.E. Marín. 1998. Salt-water intrusion and nitrate contamination in the Valley of Hermosillo and El Sahuaral coastal aquifers, Sonora, Mexico. *Hydrogeology Journal*, 6, pp. 518–526.

Steyl, G., I. Dennis. 2010. Review of coastal-area aquifers in Africa. *Hydrogeology Journal*, 18, pp. 217–225.

Szynkiewicz, A., M. Rangel-Medina, M. Modelska, R. Monreal, L.M. Pratt. 2008. Sulfur isotope study of sulfate in the aquifer of Costa de Hermosillo (Sonora, Mexico) in relation to upward intrusion of saline groundwater, irrigation pumping and land cultivation. *Applied Geochemistry*, 23, pp. 2539–2558.

Valencia-Moreno, M., J. Ruiz, L. Ochoa-Landin, R. Martinez-Serrano, P. Vargas-Navarro. 2003. Geochemistry of the Coastal Sonora batholith, Northwestern Mexico. *Canadian Journal of Earth Sciences*, 40, pp. 819–831.

Vengosh, A., J. Gill, M.L. Davisson, G.B. Hudson. 2002. A multi-isotope (B, Sr, O, H, and C) and age dating (^{3}H-^{3}He and ^{14}C) study of groundwater from Salinas Valley, California: hydrochemistry, dynamics, and contamination processes. *Water Resources Research*, 38, Doi: 10.1029/2001WR000517.

Vengosh, A., A. Starinsky, D.A. Anati. 1994a. The origin of Mediterranean interstitial waters — relics of ancient Miocene brines: A re-evaluation. *Earth and Planetary Science Letters*, 121, pp. 613–627.

Vengosh, A., A. Starinsky, Y. Kolodny, A.R. Chivas. 1994b. Boron isotope geochemistry of thermal springs from the northern Rift Valley, Israel. *Journal of Hydrology*, 162, pp. 155–169.

Werner, A.D. 2010. A review of seawater intrusion and its management in Australia. *Hydrogeology Journal*, 18, pp. 281–285.

Werner A.D., M. Bakker, V.E.A. Post, A. Vandenbohede, Ch. Lu, B. Ataie-Ashtiani, C.T. Simmons, D.A. Barry. 2013. Seawater intrusion processes, investigation and management: Recent advances and future challenges, *Advances in Water Resource*, 51, pp. 3–26.

Werner, A.D., M.R. Gallagher. 2006. Characterisation of sea-water intrusion in the Pioneer Valley, Australia using hyfrochemistry and three-dimensional numerical modeling. *Hydrogeology Journal*, 14, pp. 1452–1469.